Published in final edited form as:
Proc Hum Factors Ergon Soc Annu Meet. 2017 ; 61(1): 1046–1050. doi:10.1177/1541931213601745.

Effects of Movement Speed and Magnetic Disturbance on the Accuracy of Inertial Measurement Units

Howard Chen[1], **Mark C. Schall Jr.**[2], **Nathan Fethke**[1]

[1]University of Iowa

[2]Auburn University

Abstract

This study evaluated the effects of motion speed and magnetic disturbance on the spatial orientation accuracy of an inertial measurement unit (IMU) on the hand. Thirteen participants performed six trials of a repetitive material transfer task. Movement speed (15, 30, 45 transfers/minute) and magnetic disturbance (absent, present) were the independent variables. Optical motion capture was the reference. Root-mean-square differences (RMSD) exceeded 20° when inclination measurements (pitch and roll) were calculated using the IMU accelerometer. A linear Kalman filter and a proprietary, embedded Kalman filter reduced inclination RMSD to <3° across all movement speeds. The RMSD in the heading direction (i.e., about gravity) increased (from <5° to 17°) under magnetic disturbance. The linear Kalman filter and the embedded Kalman filter reduced heading RMSD to <12° and <7°, respectively. Use of IMUs and Kalman filters can improve inclinometer measurement accuracy. However, magnetic disturbances continue to limit the accuracy of three-dimensional IMU motion capture.

INTRODUCTION

Accelerometers have for years been used in field studies to describe the inclination of the trunk and upper arms with respect to the gravity vector (i.e., pitch angle) and the horizon (i.e., roll angle) (Åkesson, 1997; Fahrenberg, 1997). However, accelerometers (i) are most accurate when the motion to be assessed are static or quasi-static, and (ii) are unable to capture information regarding motions about the gravity vector (i.e., heading angle) (Amasay, 2009; Bernmark, 2002). Without heading angles, these sensors are not useful for measuring postures and movements of joints when a reference to gravity and the horizon cannot be reasonably assumed (e.g., flexion/extension of the wrist can occur with the wrist in any orientation with respect to gravity and the horizon. Inertial measurement units (IMUs), which package accelerometers with gyroscopes and magnetometers, are theoretically able to overcome the limitations of accelerometer-based measurement through the use of sensor fusion algorithms such as Kalman filters.

For field-based occupational ergonomics applications, IMUs are attractive due to their small size, relatively low cost, and ability to reliably capture information about worker posture and movement across full working shifts (Schall, 2015). These attributes are important, for example, when designing exposure assessment campaigns to estimate exposure to physical risk factors associated with musculoskeletal outcomes in epidemiological studies, or to facilitate quantitative evaluations of interventions. Commercial IMU-based motion capture systems are increasingly available and marketed to ergonomists. Typically, however, commercial systems use proprietary sensor fusion algorithms not well-understood by many ergonomics practitioners. Moreover, the accuracy of IMU-based motion capture remains an important issue.

Several studies have compared metrics of joint kinematics obtained using IMUs to those obtained using optical motion capture (Cloete, 2008; Kim, 2013; Robert-Lachaine, 2016; Cuesta-Vargas, 2010). For example, Cloete and Scheffer (2008) observed errors <6° for hip flexion/extension, but >15° for ankle rotation. Similarly, Godwin, et al., (2009) reported errors >20° (i) between different body segments within the same task and (ii) within the same body segment between different tasks. While these studies are immediately applicable to practitioners, error magnitudes are influenced by the biomechanical models used. Robert-Lachaine et al., (2016) observed that differences in protocol between the IMU and OMC can account for differences >40°, while the actual sensor error was <5°. In addition, the use of commercial hardware with proprietary algorithms for converting raw IMU data to kinematic constructs limits the generalizability of these studies' results beyond potentially idiosyncratic commercial solutions.

The spatial orientation of IMUs (i.e., heading, pitch and roll angles rather than kinematic variables) is often presented when (i) developing and comparing sensor fusion algorithms and (ii) assessing factors that can negatively affect IMU accuracy. Such studies have generally reported greater accuracy (<6° average error; Bergamini, 2014; Faber, 2013; Lebel, 2013; Ligorio, 2016; Ricci, 2016) than those reporting kinematic variables. Spatial orientation is theoretically obtainable with a gyroscope. However, gyroscopes built using micro-electromechanical systems and packaged with IMUs are inaccurate, leading to time-dependent error known as gyroscopic drift. Deviations >10° per minute have been observed (Bergamini, 2014; Luinge, 2007). Alternatively, IMU spatial orientation can be derived with respect to gravity and magnetic north assuming the measured acceleration is due solely to gravity and a homogenous local magnetic field (Bachmann, 2004; Ligorio, 2016). These measurements are considered time-invariant, but can be adversely affected by highly dynamic motion and fluctuations within the local magnetic field (Amasay, 2009; Bernmark, 2002; de Vries, 2009; Lebel, 2013) leading to deviations of up to 180° (Bachmann, 2004).

Sensor fusion algorithms are used to address the limitations of these two methods. Regardless of the fusion algorithm, the primary source of information is generally the gyroscope. Accelerometer and magnetometer measurements are used to remove gyroscopic drift (Yun, 2006). Dynamic and magnetic disturbances are often attenuated through increased reliance on gyroscope measurements with the expectation of time-dependent errors during periods of disturbance (Ligorio, 2016; Roetenberg, 2005; Sabatini, 2006; Sessa, 2012).

The primary objective of this pilot study was to examine the effects of movement speed and magnetic disturbance (and their interaction) on IMU spatial orientation accuracy during a repetitive upper extremity task. In order to extend generalizability, IMU spatial orientation was calculated using both non-proprietary and proprietary Kalman filter approaches. The potential benefit of estimating inclination using an IMU with sensor fusion compared to an accelerometer-only approach was also explored.

METHODS

Participants

Thirteen participants (11 male; mean age= 27.2 ± 6.6 years; right-hand dominant) were recruited from the local community. Participants self-reported no history of orthopedic surgery in the upper extremity (shoulder, elbow, wrist, and hand), no physician-diagnosed musculoskeletal disorders disorder in the past six months, and no musculoskeletal pain in the two weeks prior to enrollment. The University of Iowa Institutional Review Board approved all study procedures, and informed consent was obtained from all participants.

Experimental Task

The experimental task involved transferring wooden dowels (2 cm diameter × 8 cm length) for one minute from a waist-level container located directly in front of the participant to a shoulder-level container placed 45° diagonally with respect to the sagittal and frontal planes. Three levels of movement speed were assigned: 'slow' (15 transfers/min), 'medium' (30 transfers/min), and 'fast' (45 transfers/min). Pacing was controlled using a metronome. A metal plate (30.5 cm × 10 cm × 0.6 cm) was placed within the shoulder-level container to create a local magnetic field disturbance. Participant performed six trials of the task, once at each of the three movement speeds both with and without the metal plate. Experimental conditions were randomized to control for potential order effects. Participants were given time to acclimate to the motion speeds before each trial began. Each one-minute trial was followed by a rest period of five minutes.

Instrumentation and Data Processing

The spatial orientation of the hand was simultaneously measured using an IMU (SXT, Nexgen Ergonomics, Inc., Pointe Claire, Quebec, CA) and a six-camera OMC system (Optitrack Flex 13, NaturalPoint, Inc., Corvallis, OR, USA) that tracked a rigid marker cluster attached to the IMU surface. The IMU and OMC data were recorded at 128 Hz and 120 Hz, respectively (the maximum rates for each system). Raw IMU data at each sample included acceleration, angular velocity, and magnetic field strength (all tri-axial), as well as a quaternion rotation vector a consisting of a real component (q_0) and imaginary components (q_1, q_2, q_3) output by a proprietary, embedded Kalman filter. Raw OMC data at each sample (i.e., spatial position of the marker cluster) were converted to a quaternion rotation vector using the manufacturers' software (Motive, NaturalPoint, Inc., Corvallis, OR, USA).

The fundamental objective of all post-processing was to calculate the spatial orientation of the IMU and of the OMC marker cluster using the Euler rotation convention of heading (ψ), pitch (θ), and roll (ϕ) angles. The IMU spatial orientation was estimated with three approaches: (i) using the raw IMU data streams (i.e., acceleration, angular velocity, and magnetic field strength) without sensor fusion, (ii) using modifications of a published, non-proprietary sensor fusion algorithm, and (iii) using the quaternion output from the IMU's embedded and proprietary Kalman filter. The spatial orientation derived from the OMC marker cluster was calculated using the quaternion output of the OMC system software. All post-processing was accomplished using MATLAB (2016a, Mathworks, Natick, MA). The raw IMU data were down-sampled to 120 Hz to match the OMC sampling rate.

IMU spatial orientation: no sensor fusion.—IMU pitch (θ) and roll (ϕ) angles are calculated from the accelerometer output (a_x, a_y, a_z) using Equations 1 and 2:

$$\theta = \tan^{-1}\left(-a_x / \sqrt{a_y^2 + a_z^2}\right) \tag{1}$$

$$\phi = \tan^{-1}\left(a_y / a_z\right) \tag{2}$$

Heading angle (ψ, i.e., rotation around gravity) is calculated using the pitch and roll measurements combined with the magnetometer output (m_x,m_y,m_z) according to Equation 3:

$$\psi = \tan^{-1}\left(\frac{m_z \sin\phi - m_y \cos\phi}{m_x \cos\theta + m_y \sin\theta \sin\phi + m_z \sin\theta \cos\phi}\right) \tag{3}$$

The raw accelerometer data stream was low-pass filtered (2$^{\text{nd}}$ order Butterworth, 3 Hz corner frequency) prior to the Euler rotation angle calculations. Pitch and roll angles calculated without sensor fusion are described hereafter using the designation "Accel". Heading angles calculated using raw magnetometer measurements (m_x,m_y,m_z) are described hereafter using the designation "Mag." Heading measurements calculated using Mag contained pitch and roll measurements obtained from the non-proprietary sensor fusion algorithm to mitigate the effects of increased movement speeds on heading error.

IMU spatial orientation: non-proprietary sensor fusion.—A Kalman filter that separated the gravity vector from linear acceleration (given gyroscope and accelerometer measurements) was used to compute the acceleration magnitudes as inputs into Equations 1 and 2. Pitch and roll angles calculated in this manner are described hereafter using the designation "Accel-KF." Similarly, a Kalman filter that separated the magnetic north vector from transient magnetic field strength fluctuation (given gyroscope and magnetometer measurements) was used to compute the magnetic field strength magnitudes as inputs into Equation 3. Heading angles calculated in this manner are described hereafter using the designation "Mag-KF." These Kalman filters were direct implementations of the "Linear Kalman Filter" proposed by Ligorio & Sabatini (2015) and later extended to account for magnetic disturbance (Ligorio, 2016). This specific filter was chosen based on simplicity of design and implementation. The filter tuning parameters (Table 1) were derived experimentally.

IMU spatial orientation: embedded Kalman filter.—Equation 4 was used to convert the quaternion rotation vector output from the IMU's embedded Kalman filter to heading, pitch, and roll angles. The angles calculated in this manner are described hereafter with the designation "Em-KF."

$$\begin{bmatrix}\psi\\ \theta\\ \phi\end{bmatrix}=\begin{bmatrix}\tan^{-1}\left(2(q_0q_3+q_1q_2)/\left(q_0^2+q_1^2-q_2^2-q_3^2\right)\right)\\ \sin^{-1}(2(q_0q_2-q_1q_3))\\ \tan^{-1}\left(2(q_0q_1+q_2q_3)/\left(q_0^2-q_1^2-q_2^2+q_3^2\right)\right)\end{bmatrix} \quad (4)$$

OMC marker cluster spatial orientation.—The raw OMC orientation measurements were first low-pass filtered (2nd order Butterworth, 6 Hz corner frequency). Then the quaternion rotation vector output from the OMC system software was converted to heading, pitch, and roll angles using Equation 4.

Error calculation.—The offset between the local coordinate frames of the OMC and the IMU was calculated using angular rate measurements according to de Vries et al. (2010). After applying the local offset, the offset between the global coordinate frames of the OMC and the IMU was determined under static conditions using IMU-derived orientation using the Mag approach. For each trial, the root-mean-square difference (RMSD) between the IMU- and OMC-derived heading, pitch, and roll angles was calculated as:

$$RMSD_{\vartheta}=\sqrt{\frac{1}{n}\sum_{i=1}^{n}\left(\vartheta_{OMC,i}-\vartheta_{IMU,i}\right)^2} \quad (5)$$

where i is the sample number, n is the number of samples, and ϑ_{OMC} and ϑ_{IMU} are the Euler rotation angles measured by the OMC and IMU, respectively.

Statistical Analysis

Two-factor repeated measures analyses of variance were used to estimate the effects of movement speed, magnetic disturbance, and their interaction on estimates of RMSD in the heading, pitch, and roll directions. The Greenhouse-Geisser correction was used to adjust for violations of sphericity. All statistical analyses were performed using SPSS Statistics 23 (IBM, SPSS, Chicago, Illinois, USA).

RESULTS

RMSD in the Pitch and Roll Directions

Regardless of the IMU spatial orientation estimation approach, neither the main effect of magnetic disturbance nor the interaction between movement speed and magnetic disturbance on RMSD was significant in the pitch and roll directions. The main effect of movement speed on RMSD in pitch and roll, however, was significant for the Accel and Accel-KF approaches but not for the Em-KF approach (Table 2). In general, mean RMSD increased with increasing movement speed; large increases (4° during the ‘slow’ condition to 24° during the ‘fast’ condition) were observed when using the Accel approach and small increases (1.1° to 1.9°) when using the Accel-KF approach. For the ‘medium’ and ‘fast’ movement speeds, using a Kalman filter (i.e., either the Accel-KF or Em-KF approach) to estimate pitch and roll reduced RMSD by an order of magnitude compared to using only the accelerometer (i.e, the Accel approach). Sample-to-sample differences between OMC and IMU pitch measurements were not time-dependent (Figure 1).

RMSD in the Heading Direction

For one participant, the heading RMSD from two trials processed using the Em-KF approach was more than four standard deviations greater than the mean heading angle RMSD across all subjects and testing conditions. These measurements were considered outliers and discarded from the analysis. Regardless of the IMU spatial orientation estimation approach, neither the main effect of movement speed nor the interaction between movement speed and magnetic disturbance on RMSD was significant in the heading direction. The main effect of magnetic disturbance on RMSD in the heading direction was significant for Mag, confirming that the metal plate altered the local magnetic field. The metal plate also adversely affected heading angle RMSD for both sensor fusion algorithms (Mag-KF, and Em-KF) (Table 3) although the proprietary Em-KF performed somewhat better than the non-proprietary Mag-KF. Sample-to-sample differences between OMC and IMU heading measurements were time-dependent when using sensor fusion, particularly the Em-KF (Figure 2).

DISCUSSION

Consistent with other studies, pitch and roll angles estimated using only an accelerometer were less accurate as movement speed increased (Korshøj, 2014). This is primarily a function of increased tangential and centripetal acceleration magnitudes (Bernmark, 2002). While the accuracy of pitch and roll using the Accel-KF approach was influenced by movement speed, the magnitude of mean RMSD between the ‘slow’ and ‘fast’ movement speed was negligible (<1°). Both sensor fusion algorithms reduced RMSD in the pitch and roll directions to <3°across all movement speed conditions, which is consistent with previous studies (Bergamini, 2014; Ligorio, 2015, 2016). This finding suggests that IMU-derived inclination measurements improved measurement accuracy compared to accelerometer-derived inclination measurements commonly used to quantify non-neutral postures in the workplace within the context of occupational ergonomics.

The mean RMSD in the heading direction in testing conditions without the metal plate (<5° RMSD) was consistent with previous studies (<6°) (Bergamini, 2014; Faber, 2013; Lebel, 2013; Ligorio, 2016). As anticipated, the presence of the metal plate degraded the heading angle accuracy, though to a lesser extent when sensor fusion was used. We suspect that the addition of magnetic disturbance compensation strategies (e.g., vector selection) would improve measurement accuracy under the presence of magnetic disturbance. However, it is unlikely that sensor fusion algorithms would eliminate magnetic disturbances as long as magnetometers remain as a source of information regarding orientation about the gravity vector.

CONCLUSION

The use of IMUs in field-based ergonomics research is expected to increase as hardware development accelerates and more commercial options are available. We did not observe an interaction between movement speed and magnetic disturbance on the accuracy of IMU spatial orientation in this study. We observed substantially greater accuracy in IMU pitch and roll angles when using sensor fusion compared to using an accelerometer alone. This finding is important, as it suggests the increase in technical complexity when using an IMU with sensor fusion (vs. an accelerometer only) is offset by meaningful improvements in measurement accuracy for describing the postures and movements of certain body segments in dynamic situations with fast motion speeds. Another key observation is that the non-proprietary Kalman filters used in this study performed similarly to the embedded, proprietary Kalman filter packaged with the IMU hardware (although somewhat poorer with magnetic disturbance). Making such open-source processing alternatives available to the ergonomics community can, over time, reduce the reliance on proprietary solutions and improve the comparability of IMU-based research. We plan to make our algorithms available in the near future. Finally, the full potential of IMU-based motion capture for field research is not likely to be realized without methods to identify and/or minimize the effects of local magnetic field disturbances.

ACKNOWLEDGMENTS

This research was supported (in part) by a pilot project research training grant from the Heartland Center for Occupational Health and Safety at the University of Iowa. The Heartland Center is supported by Training Grant No. T42OH008491 from the Centers for Disease Control (CDC) and Prevention/National Institute for Occupational Safety and Health (NIOSH).

REFERENCES

Akesson I, Hansson G-Å, Balogh I, Moritz U, & Skerfving S (1997). Quantifying Work Load in Neck, Shoulders and Wrists in Female Dentists. International Archives of Occupational and Environmental Health, 69(6), 461–474. [PubMed: 9215934]

Amasay T, Zodrow K, Kincl L, Hess J, & Karduna A (2009). Validation of Tri-Axial Accelerometer for the Calculation of Elevation Angles. International Journal of Industrial Ergonomics, 39(5), 783–789.

Bachmann ER, Yun X, & Peterson CW (2004). An Investigation of the Effects of Magnetic Variations on Inertial/Magnetic Orientation Sensors. In 2004 IEEE International Conference on Robotics and Automation, 2004. Proceedings. ICRA ‘04 (Vol. 2, p. 1115–1122 Vol.2).

Bergamini E, Ligorio G, Summa A, Vannozzi G, Cappozzo A, & Sabatini AM (2014). Estimating Orientation Using Magnetic and Inertial Sensors and Different Sensor Fusion Approaches: Accuracy Assessment in Manual and Locomotion Tasks. Sensors, 14(10), 18625–18649. [PubMed: 25302810]

Bernmark E, & Wiktorin C (2002). A Triaxial Accelerometer for Measuring Arm Movements. Applied Ergonomics, 33(6), 541–547. [PubMed: 12507338]

Cloete T, & Scheffer C (2008). Benchmarking of a Full-Body Inertial Motion Capture System for Clinical Gait Analysis. In 2008 30th Annual International Conference of the IEEE Engineering in Medicine and Biology Society (pp. 4579–4582).

Cuesta-Vargas AI, Galán-Mercant A, & Williams JM (2010). The Use of Inertial Sensors System for Human Motion Analysis. Physical Therapy Reviews, 15(6), 462–473. [PubMed: 23565045]

de Vries WHK, Veeger HEJ, Baten CTM, & van der Helm FCT (2009). Magnetic Distortion in Motion Labs, Implications for Validating Inertial Magnetic Sensors. Gait & Posture, 29(4), 535–541. [PubMed: 19150239]

Faber GS, Chang C-C, Rizun P, & Dennerlein JT (2013). A Novel Method for Assessing the 3-D Orientation Accuracy of Inertial/Magnetic Sensors. Journal of Biomechanics, 46(15), 2745–2751. [PubMed: 24016678]

Fahrenberg J, Foerster F, Smeja M, & Müller W (1997). Assessment of Posture and Motion by Multichannel Piezoresistive Accelerometer Recordings. Psychophysiology, 34(5), 607–612. [PubMed: 9299915]

Godwin A, Agnew M, & Stevenson J (2009). Accuracy of Inertial Motion Sensors in Static, Quasistatic, and Complex Dynamic Motion. Journal of Biomechanical Engineering, 131(11), 114501–

Kim S, & Nussbaum MA (2013). Performance Evaluation of a Wearable Inertial Motion Capture System for Capturing Physical Exposures During Manual Material Handling Tasks. Ergonomics, 56(2), 314– [PubMed: 23231730]

Korshøj M, Skotte JH, Christiansen CS, Mortensen P, Kristiansen J, Hanisch C, … Holtermann A (2014). Validity of the Acti4 Software Using Actigraph Gt3x+accelerometer for Recording of Arm and Upper Body Inclination in Simulated Work Tasks. Ergonomics, 57(2), 247–253. [PubMed: 24392673]

Lebel K, Boissy P, Hamel M, & Duval C (2013). Inertial Measures of Motion for Clinical Biomechanics: Comparative Assessment of Accuracy under Controlled Conditions - Effect of Velocity. PLOS ONE, 8(11), e79945.

Ligorio G, Bergamini E, Pasciuto I, Vannozzi G, Cappozzo A, & Sabatini AM (2016). Assessing the Performance of Sensor Fusion Methods: Application to Magnetic-Inertial-Based Human Body Tracking. Sensors, 16(2), 153. [PubMed: 26821027]

Ligorio G, & Sabatini AM (2015). A Novel Kalman Filter for Human Motion Tracking With an Inertial-Based Dynamic Inclinometer. IEEE Transactions on Biomedical Engineering, 62(8), 2033–2043. [PubMed: 25775483]

Ligorio G, & Sabatini AM (2016). Dealing with Magnetic Disturbances in Human Motion Capture: A Survey of Techniques. Micromachines, 7(3), 43.

Luinge HJ, Veltink PH, & Baten CTM (2007). Ambulatory Measurement of Arm Orientation. Journal of Biomechanics, 40(1), 78–85. [PubMed: 16455089]

Ricci L, Taffoni F, & Formica D (2016). On the Orientation Error of IMU: Investigating Static and Dynamic Accuracy Targeting Human Motion. PLOS ONE, 11(9), e0161940.

Robert-Lachaine X, Mecheri H, Larue C, & Plamondon A (2016). Validation of inertial measurement units with an optoelectronic system for whole-body motion analysis. Medical & Biological Engineering & Computing, 1–11.

Roetenberg D, Luinge HJ, Baten CTM, & Veltink PH (2005). Compensation of Magnetic Disturbances Improves Inertial and Magnetic Sensing of Human Body Segment Orientation. IEEE Transactions on Neural Systems and Rehabilitation Engineering, 13(3), 395–405. [PubMed: 16200762]

Sabatini AM (2006). Quaternion-Based Extended Kalman Filter for Determining Orientation by Inertial and Magnetic Sensing. IEEE Transactions on Biomedical Engineering, 53(7), 1346–1356. [PubMed: 16830938]

Schall MC Jr., Fethke NB, Chen H, Oyama S, & Douphrate DI (2015). Accuracy and Repeatability of an Inertial Measurement Unit System for Field-Based Occupational Studies. Ergonomics, 1–12.

Sessa S, Zecca M, Lin Z, Bartolomeo L, Ishii H, & Takanishi A (2012). A Methodology for the Performance Evaluation of Inertial Measurement Units. Journal of Intelligent & Robotic Systems, 71(2), 143–157.

Yun X, & Bachmann ER (2006). Design, Implementation, and Experimental Results of a Quaternion-Based Kalman Filter for Human Body Motion Tracking. IEEE Transactions on Robotics, 22(6), 1216–1227.

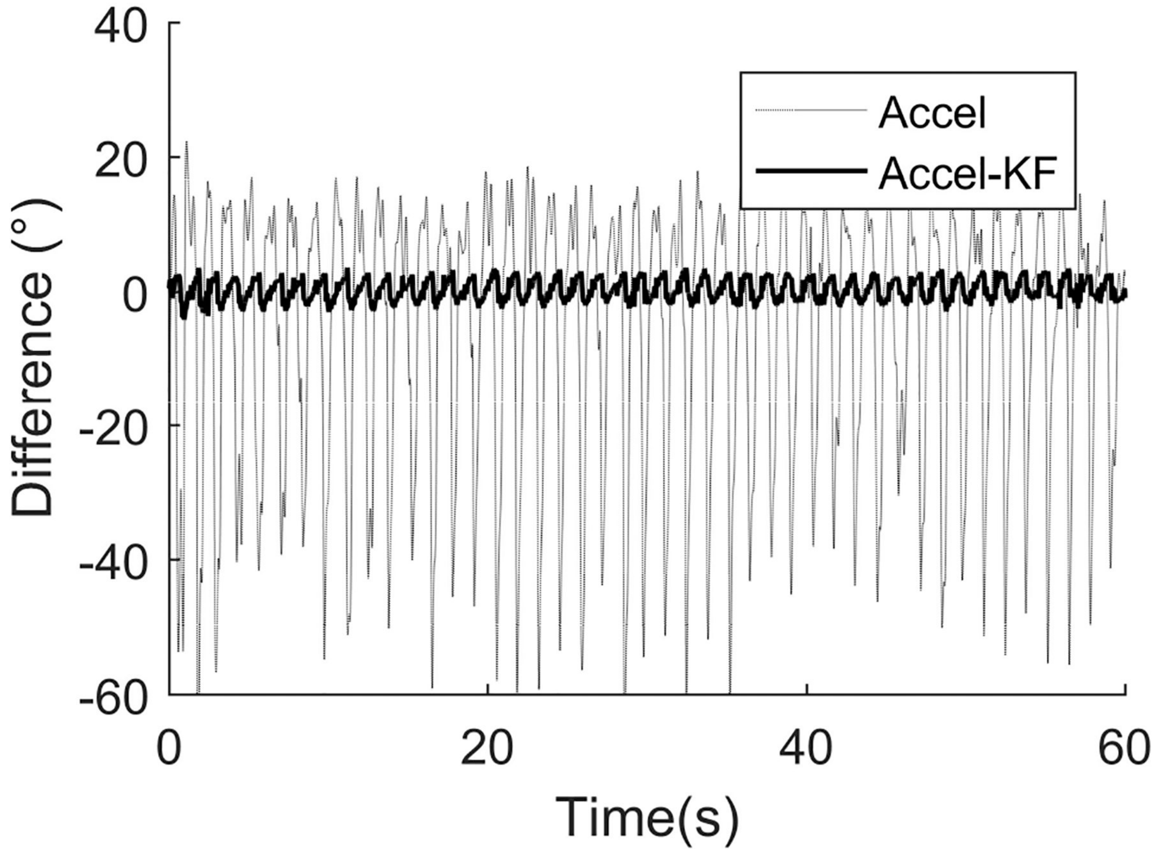

Figure 1.

Sample-to-sample difference between OMC and IMU-derived pitch measurements during the ‘fast’ movement speed condition; IMU pitch angle estimated using the accelerometer data only (Accel) and a linear Kalman filter (Accel-KF)

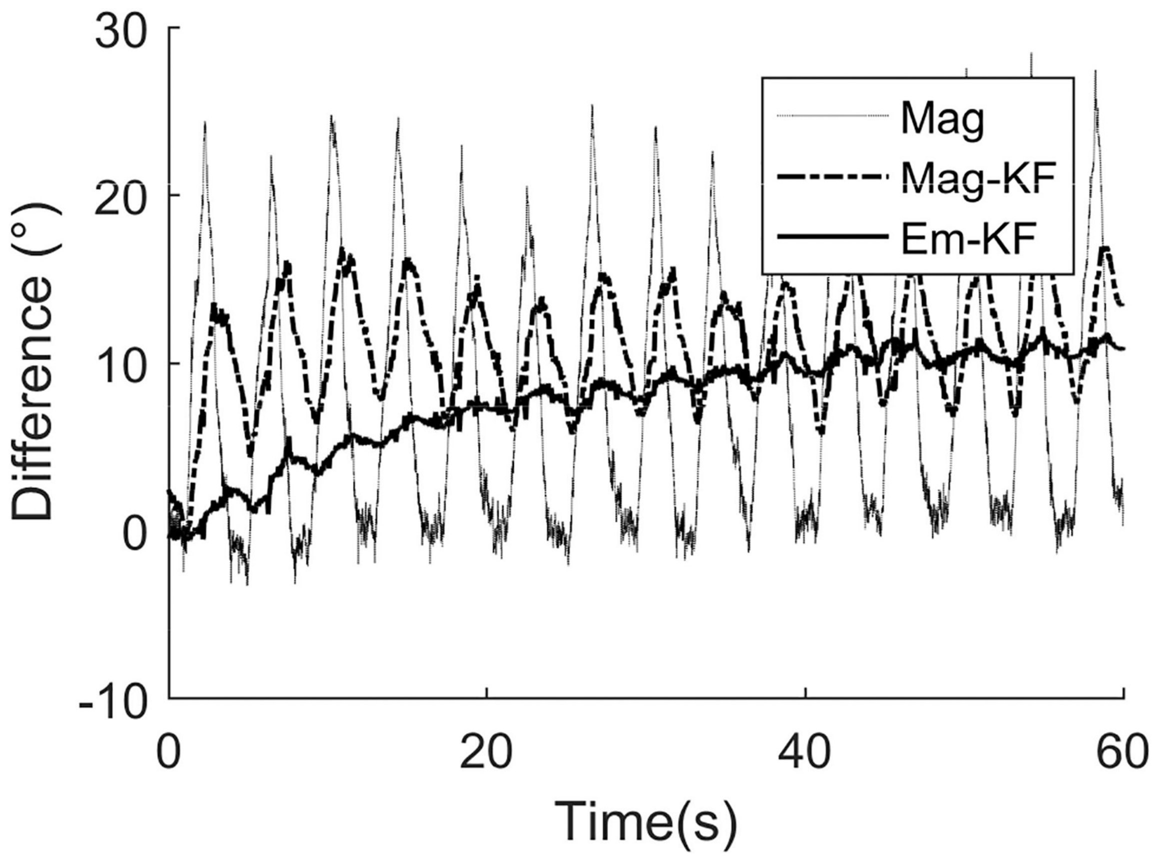

Figure 2.

Sample-to-sample difference between OMC and IMU-derived heading measurements during the 'slow' movement speed; IMU heading angle was estimated using the magnetometer only (Mag), a linear Kalman filter (Mag-KF) and a proprietary embedded Kalman filter (Em-KF).

Table 1.

Kalman filter parameters.

	Process Noise	**Meas. Noise**	c_a	c_b
Accel-KF	0.005 rad/s	0.008 m/s^2	0.3	0.08
Mag-KF	0.005 rad/s	0.3 μT	0.1	0.5

Gauss-Markov parameters $\mathbf{c_a}$ and $\mathbf{c_b}$ are tuning parameters that determine the separation of vector measurements (e.g., gravity) from transient fluctuations (e.g., linear acceleration).

Table 2.

Mean (SD) root-mean-square differences in pitch and roll (°) calculated using an accelerometer (Accel), a linear Kalman filter (Accel-KF) and an embedded proprietary Kalman Filter (Em-KF).

	Slow	Med	Fast	*p*-value
Pitch				
Accel	4.0(0.7)	11.3(1.7)	24.0(2.5)	<0.01
Accel-KF	1.1(0.5)	1.5(0.5)	1.9(0.4)	<0.01
Em-KF	1.5(0.8)	1.8(1.2)	1.7(0.9)	
Roll				
Accel	3.1(0.8)	6.4(1.7)	12.6(3.8)	<0.01
Accel-KF	1.0(0.5)	1.4(0.5)	1.5(0.5)	<0.01
Em-KF	2.2(1.4)	2.6(2.1)	2.1(1.4)	

Table 3.

Mean (SD) root-mean-square difference in heading (°) calculated using a magnetometer (Mag), a linear Kalman filter (Mag-KF) and an embedded proprietary Kalman Filter (Em-KF).

	w/o Metal	**w/Metal**	***p*-value**
Mag	3.3(1.0)	17.0(4.5)	<0.01
Mag-KF	4.1(1.9)	11.6(4.0)	<0.01
Em-KF	4.3(2.1)	7.0(4.1)	<0.05